Production of K^+ Mesons in 2.85- and 2.40-BeV p-p Collisions*

J. T. Reed,†‡ A. C. Melissinos,† N. W. Reay,†§ and T. Yamanouchi†
Department of Physics and Astronomy, University of Rochester, Rochester, New York

AND

E. J. Sacharidis,‖ S. J. Lindenbaum, S. Ozaki, and L. C. L. Yuan
Brookhaven National Laboratory, Upton, New York

(Received 4 December 1967)

We report an experimental measurements of K^+-meson production in p-p collisions at 2.85 and 2.40 BeV. The momentum spectra of the K^+ mesons are given at the three laboratory angles of 0°, 17°, and 32°. The K^+ mesons were identified by momentum and velocity using differential Čerenkov counters with a combined rejection of the order of 10^{-6}. It is shown that the production spectra can be accounted for by a one-meson-exchange mechanism with the introduction of appropriate cutoffs. At the high-energy limit of the 0° spectrum, a clear peak is observed, which is attributed to the low-energy Λ-p interaction in the $K\Lambda p$ final state. No other enhancements or pronounced effects due to resonances either in the Yp or KY system are observed.

I. INTRODUCTION

In this paper we report on an experiment to measure the production of K^+ mesons in p-p collisions at Cosmotron energies ($T_p<3$ BeV). In this energy region K mesons are produced almost entirely in association with a hyperon through the interactions

$$p+p\rightarrow p+\Lambda^0+K^+, \quad (1)$$

$$p+p\rightarrow p+\Sigma^0+K^+, \quad (2)$$

$$p+p\rightarrow n+\Sigma^++K^+. \quad (3)$$

Four-body final states including π^+ or π^0 production contribute a small fraction of approximately 15% to the total yield. The production of K-meson pairs through

$$p+p\rightarrow p+p(n)+K^++K^-(\bar{K}^0) \quad (4)$$

is strongly suppressed (see Sec. III D).

This work is the completion of a program initiated by Lindenbaum and Yuan[1–3] designed to investigate by counter techniques meson-production processes in p-p and p-nucleus collisions. As was done in previous experiments, the external proton beam of the Cosmotron was made incident on a liquid-hydrogen target, and the K mesons produced at 0°, 17°, and 32° in the laboratory were momentum-analyzed by means of magnetic spectrometers and identified by a combination of Čerenkov and scintillation counters.

The present experiment was performed at the Brookhaven Cosmotron. Preliminary results on the production of K mesons have been reported.[4] With the same apparatus we also obtained additional data on π-meson production at incident proton energies $T_p=2.00$ and 2.40 BeV; these have been published by Reay *et. al.*[5]

Strange-particle production in p-p collisions has been studied using hydrogen bubble chambers[6–8] for $T_p=2.85$, $T_p=4.10$, and $T_p=4.60$ BeV. By such techniques it is possible to distinguish among different production channels so as to obtain partial cross sections as well as the correlation spectra between the final-state particles. In counter experiments, on the other hand, better statistics can be accumulated; we therefore have measured the doubly differential production cross section $d^2\sigma/d\Omega dp$, namely, the momentum spectrum at fixed laboratory angle. The good statistics permitted us to detect in the 0° beam the effect of the low-energy Λ-p interaction.[4]

In what follows we discuss in Sec. II the beams and detection equipment. In Sec. III we present our results and compare them with the predictions of the one-meson-exchange model.[9] Finally, in Sec. IV, the effects of the low-energy Λ-p interaction on our data are analyzed and discussed in some detail.

* Work supported by the U. S. Atomic Energy Commission under contract No. AT-875-UR.

† During the performance of this experiment, these authors held guest appointments at Brookhaven National Laboratory.

‡ Part of this work is the subject of a thesis submitted by J. T. Reed in partial fulfillment of the requirements of the Doctor of Philosophy degree at the University of Rochester. Present address: Eastman Kodak Co., Rochester, New York.

§ Present address: Ohio State University, Columbus, Ohio.

‖ Present address: CERN, Geneva, Switzerland.

[1] S. J. Lindenbaum and L. C. L. Yuan, Phys. Rev. **93**, 1431 (1954); **103**, 404 (1956).

[2] S. J. Lindenbaum and L. C. L. Yuan, Phys. Rev. **105**, 1931 (1957).

[3] A. C. Melissinos, T. Yamanouchi, G. G. Fazio, S. J. Lindenbaum, and L. C. L. Yuan, Phys. Rev. **128**, 2373 (1962).

[4] A. C. Melissinos, N. W. Reay, J. T. Reed, T. Yamanouchi, E. Sacharidis, S. J. Lindenbaum, S. Ozaki, and L. C. L. Yuan, Phys. Rev. Letters **14**, 604 (1965).

[5] N. W. Reay, A. C. Melissinos, J. T. Reed, T. Yamanouchi, and L. C. L. Yuan, Phys. Rev. **142**, 918 (1966).

[6] R. I. Louttit, T. W. Morris, D. C. Rahm, R. R. Rau, A. M. Thorndike, N. J. Willis, and R. M. Lea, Phys. Rev. **123**, 1465 (1961).

[7] E. Bierman, A. P. Colleraine, and U. Nauenberg, Phys. Rev. **147**, 922 (1966).

[8] G. Alexander, O. Benary, G. Czapek, B. Haber, N. Kidron, B. Reuter, A. Shapira, E. Simopoulou, and G. Yekutieli, Phys. Rev. **154**, 1284 (1967).

[9] E. Ferrari and F. Selleri, Nuovo Cimento Suppl. **24**, 453 (1962).

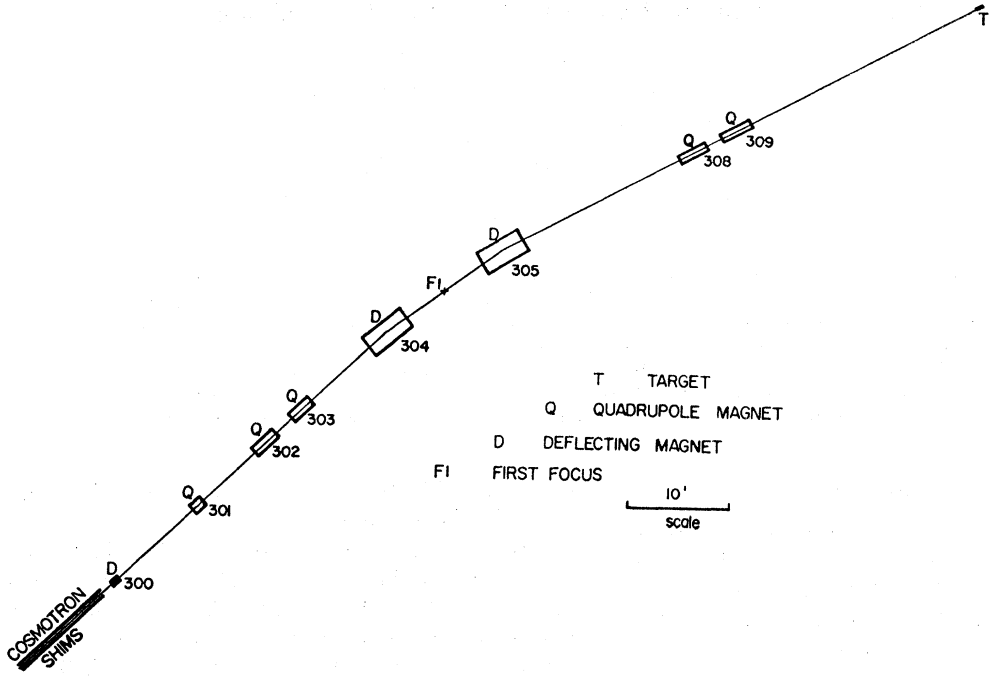

(a)

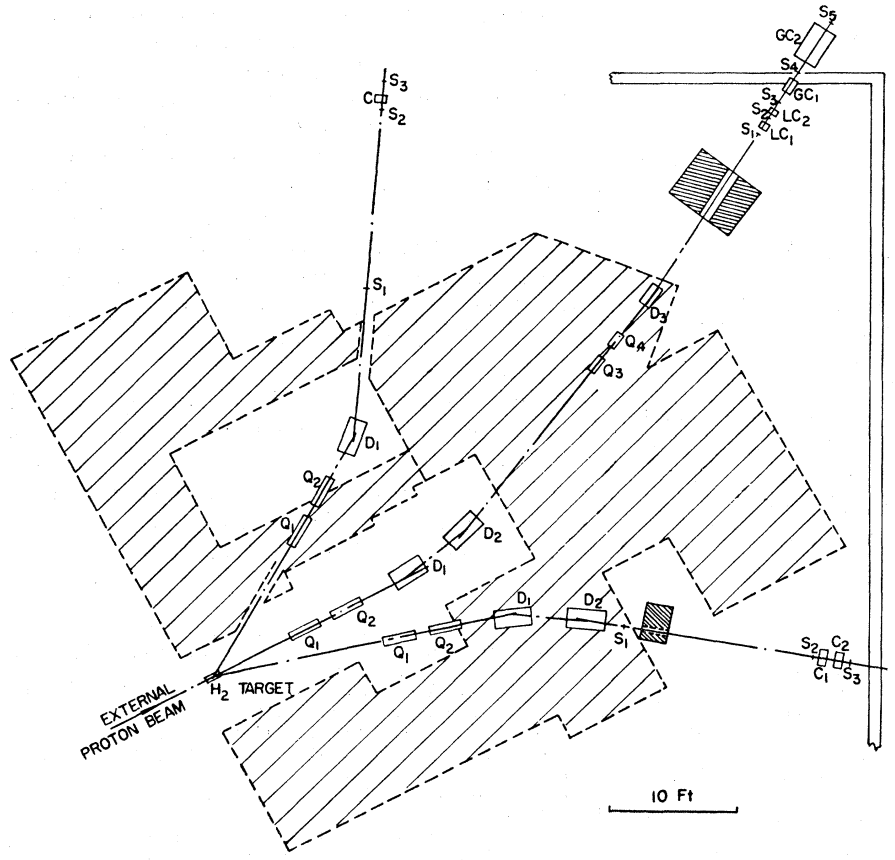

(b)

FIG. 1. Layout of the experimental beams. (a) The external proton beam III of the Cosmotron from the shims to the target. (b) The three experimental spectrometers consisting of dipoles and quadrupoles. The spectrometer angles are 0°, 17°, and 32°, respectively. The shaded area represents shielding.

II. EXPERIMENTAL ARRANGEMENT

A. Beams and Spectrometers

In this experiment the external beam No. 3 of the Brookhaven Cosmotron was used. In Fig. 1(a), the beam-transport system from the Cosmotron exit to the liquid-hydrogen target is shown. Some pertinent characteristics of the beam are given in Table I. The low spread in energy is due to the improved "flat top" of the Cosmotron, a feature of particular value to all high-resolution experiments.[10]

The target was of standard design, consisting of a 3-in.-diam cylinder with a length of 12 in. along the beam line. The secondary-beam spectrometers are shown in Fig. 1(b). They were permanently constructed at 0°, 17°, and 32° with respect to the incident beam. The focusing (quadrupole) and analyzing (dipole) elements were built into the main shielding, which was necessary to reduce the general background resulting from the primary beam, especially at its downstream stopper. The quadrupole aperture was 8 in., and for the dipoles it was 6 in.; the beam path was in vacuum wherever possible.

In the 17° and 32° beams a point-to-point focus was used. At 0° the beam was made from a point to parallel by use of Q_1 and Q_2; it passed through D_1D_2 almost parallel and was refocused by Q_3 and Q_4 to a point in the middle of the detectors. The function of the dipole D_3 was to provide an additional stage of momentum analysis in order to eliminate primary-beam protons scattered through the edges of the shielding; this was extremely important, since for protons of $T_p=2.85$ BeV, $\beta=0.969$, which is the same β as for 1.920-BeV/c K^+ mesons. Some of the characteristics of the secondary beams are summarized in Table II.

B. Detectors

The basic scheme for detection of K mesons was velocity selection, which, combined with the momentum established by the spectrometer, identifies the mass of the particle. Velocity selection was achieved with differential Čerenkov counters. At the higher momenta gas radiators[11] were used, whereas for the lower momenta the radiators were liquid cells[12]; below 1 BeV/c (in the 32° beam), time of flight was also used. Table III gives a summary of the different types of velocity selector used.

From Table II it is evident that an extremely good rejection was required, of the order of 10^5. (In the 0° beam a factor of 10^6 or better is necessary.) Thus two Čerenkov counters in coincidence (in series) were used. Equally important is an exact knowledge of the efficiency of the combined counters. To measure the latter, a third Čerenkov counter was introduced, and from the ratio $\epsilon_K=CLK/CL$ the efficiency of counter K could be obtained. CL represents the coincident count of Čerenkov counters C and L, whereas CLK is the coincident count of Čerenkov counters C, L, and K, etc.

These features of the velocity-selection system can be seen from the typical curves in Fig. 2 which pertain to the 0° beam. In Fig. 2(a) is shown the yield of the combined CK count as a function of the pressure[13] in counter K at a momentum of 1.8 BeV/c. In Fig. 2(b) is shown the yield of the combined CLK count for optimum setting of all three counters C, L, and K when the

TABLE I. Some characteristics of the external proton beam.

Flux on target per pulse	5×10^{10}
Repetition rate	12 pulses/min
Spill time	200 msec
Energy spread at $T_p=2.85$ BeV	3–5 MeV
Image size at target (vertical×horizontal)	$1\times\frac{3}{4}$ in.
Angular divergence at target (vertical, horizontal)	±6, ±7 mrad
Ejection efficiency	~30%

TABLE II. Characteristics of the secondary-beam spectrometers.

	0°	17°	32°
Horizontal magnification	2.4	5	0.8
Vertical magnification	3.0	8.5	2.9
Angular acceptance (sr)	3×10^{-4}	1.2×10^{-4}	1.1×10^{-4}
Momentum resolution dp/p	±0.6%	±1.5%	±1.2%
Defining counter (diam) (in.)	1	1	$1\frac{1}{2}$
Typical K^+ flux/pulse	3	1	0.3
Typical total flux/pulse	4×10^4	10^3	350
Target-to-focus distance (in.)	850	535	593
Effective acceptance $\epsilon\Delta\Omega\Delta p/p$ (*including* beam and detector width) (sr)	3.3×10^{-6}	8.2×10^{-7}	1.5×10^{-6}
Decay correction (typical)			
p_k 2 BeV/c	4.4		
p_k 1 BeV/c	15[a]	6.2	7.7

[a] The length to the last defining counter element is less than at the higher momenta.

TABLE III. Characteristics of the velocity-selection systems.

0° spectrometer	
Momentum range (BeV/c)	
2.2 –1.65	Counter K[a]
1.65–1.50	Counters K and C[b]
1.50–1.05	Counters C and L[c]
1.05–0.80	Counters L and J[c]
17° spectrometer	
Two liquid-radiator counters	
32° spectrometer	
One liquid-radiator counter and time of flight	

[a] K is a high-pressure CO_2 differential Čerenkov counter of 4-in.-diam useful aperture and 48 in. long. It was built by Dr. T. F. Kycia (Ref. 11).
[b] C is a high-pressure CO_2 differential Čerenkov counter of 2-in. useful aperture and 15 in. long.
[c] L and J are liquid-radiator differential Čerenkov counters of $1\frac{1}{2}$-in. useful aperture and 4 in. long, as described in Ref. 12. Similar counters were used in the 17° and 32° spectrometers.

[10] A fluorescent screen placed in front of the liquid-hydrogen target was viewed by a television camera in order to monitor the beam-spot size and position.
[11] Two high-pressure CO_2 differential Čerenkov counters were used. One was built by Dr. T. Kycia and the other at the University of Rochester. The Čerenkov angle was of the order $\theta\sim9°$. For more details see Table III.
[12] S. Ozaki, J. J. Russell, E. J. Sacharidis, L. C. L. Yuan, and J. T. Reed, Nucl. Instr. Methods **35**, 301 (1965).
[13] The pressure in counter C was also appropriately varied.

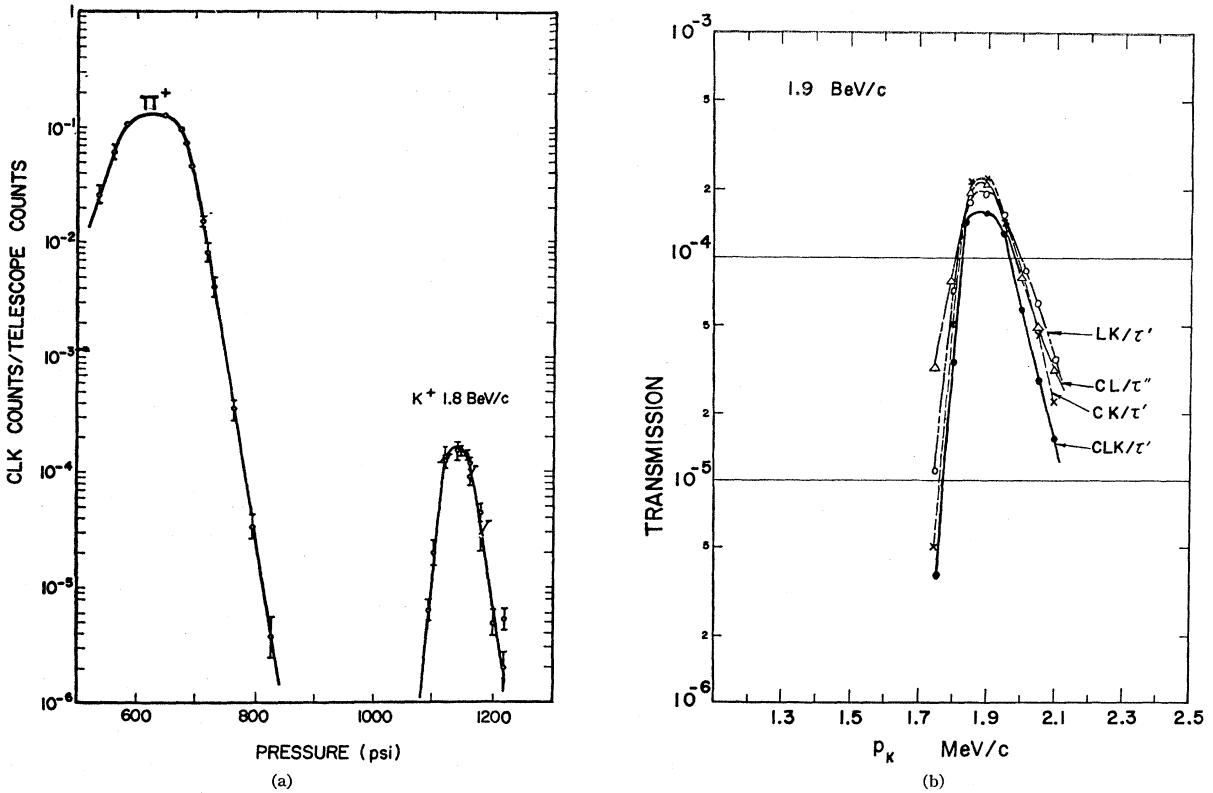

FIG. 2. Resolution curves for combined Čerenkov counters. (a) Counting rate as a function of CO_2 pressure in counter K. (b) Counting rate as a function of spectrometer momentum for fixed pressure in counters (see Table III).

spectrometer momentum was varied. Also indicated is the yield of the individual LK, CL, and CK coincidence rates. The ratio of the triple coincidence to the doubles gives the efficiency of the respective counter; the combined efficiency of CLK varied from 55 to 85%. A small correction, never exceeding 10%, had to be made in some instances for background (feed-through) counts even in the CLK coincidence. Accidental coincidences were monitored continuously and were less than 2%.

In the 32° beam a time-of-flight system was also used. The two counters were separated by 15 ft, and the output of the time-to-pulse-height converter[14] was displayed on a 400-channel RIDL analyzer. In Fig. 3(a) is shown the resulting time spectrum at a momentum of 740 MeV/c. When the input to the converter circuit was gated by a Čerenkov counter (liquid-radiator cell), the spectrum shown in Fig. 3(b) was obtained instead. Thus a clear separation of K mesons from the pions could be achieved; the efficiency of the Čerenkov counter was obtained as explained before, and also by passing protons of the appropriate velocity[15] through the system whenever this was possible.

Solid-angle and momentum-band definition was obtained with circular scintillation counters as also indicated in Table II. The electronics consisted both of the standard commercial Chronetic units[14] as well as of the Brookhaven nanocards.[16]

C. Scattering and Absorption in Detector Elements

In view of the high pressure of the radiator gas required for identifying K mesons in our momentum range, the detector presented a substantial amount of material in the path of the beam. This material results in loss of particles due both to nuclear absorption and to multiple scattering. In view of the importance of this effect, we calculated it and also measured it experimentally. For the absorption we computed an average interaction cross section per nucleon[17] ranging from 15.0 mb at 1.0 BeV/c to 18.0 mb at 2.0 BeV/c. For the multiple scattering we used (and extended) the formulas of Steinheimer.[18]

Experimentally, we measured the transmission of pions and protons through the detection system as a function of gas pressure. The results for the 0° beam are shown in Fig. 4, where the transmission at a momentum of 2.0 BeV/c is plotted versus gas density. A

[14] Manufactured by Chronetics, Inc., 500 Nuber Ave., Mt. Vernon, N. Y.

[15] Since $p=m\beta\gamma$, two particles have equal β when their momenta are in the same ratio as their masses.

[16] W. A. Higginbotham, F. Merritt, and R. Sugarman, Brookhaven National Laboratory Report No. BNL-711(T-248) (unpublished).

[17] V. S. Barashenkov and V. M. Maltsev, Fortschr. Physik **9**, 549 (1961). See p. 580.

[18] R. M. Sternheimer, Rev. Sci. Instr. **25**, 1070 (1954).

good fit can be obtained by a straight line corresponding to 23.5 mb/nucleon. We believe this to be a fair representation of the attenuation losses of K mesons and have corrected our data accordingly.

D. Momentum Resolution, Solid-Angle Calculation, and Normalization Procedure

To obtain absolute production cross sections, we need the effective acceptance $\epsilon\Delta\Omega\Delta p$ of the spectrometer as a function of momentum. $\Delta\Omega$ is the solid angle subtended by the quadrupoles and accepted by the defining detector, and $\Delta p/p$ is the relative momentum acceptance for a point source located at the center of the target; ϵ is then the efficiency resulting from averaging these quantities over the entire length of the target. Clearly, the "momentum resolution" dp/p is larger or equal to the relative momentum acceptance $\Delta p/p$.

To a good approximation the product $\epsilon\Delta\Omega\Delta p/p$ is a constant over the entire momentum range and can be obtained from the optical properties of the spectrometer. As an example, we show in Fig. 5 the results of such a calculation for the 0° beam. Figure 5(a) is a trace of a horizontal and of a vertical ray through the 0° spectrometer. From these rays one can obtain the phase-space diagram shown in Fig. 5(b) (for the horizontal plane); here we plot the limits of momentum variation and horizontal emission angle for particles originating from a point target but allowed to reach a detector of finite width (1 in.). The theoretical momentum resolution is then clearly determined by the limiting horizontal ray.

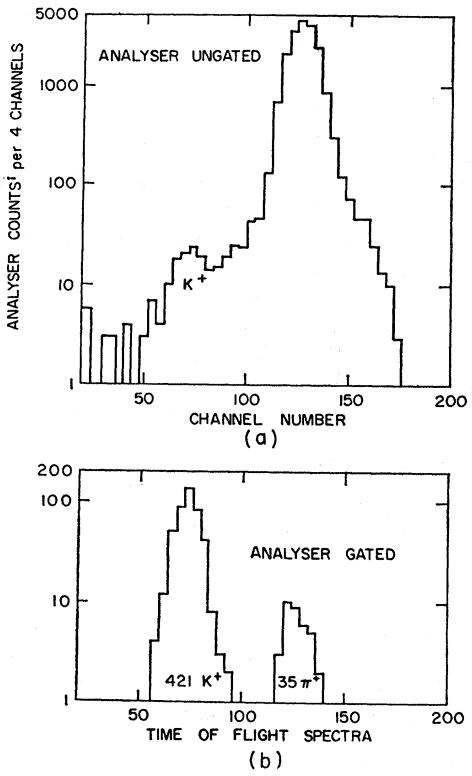

FIG. 3. Time-of-flight spectra obtained in the 32° beam at 740 MeV/c. The time scale is 20 channels equal 1 nsec. (a) The converter is not gated. (b) The converter is gated by a liquid-radiator Čerenkov counter.

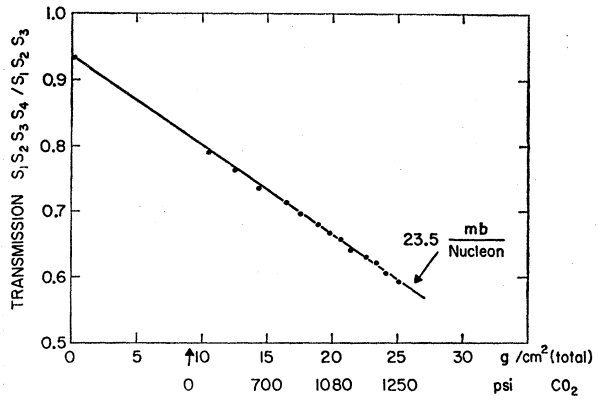

FIG. 4. The experimentally observed transmission ratio through Čerenkov counter C as a function of the total material in the beam path. A 2.0-BeV/c positive beam was incident, and the pressure of the CO_2 in the counter is also indicated. The solid line is the attenuation expected to first order from a total interaction cross section of 23.5 mb/nucleon.

The solid curve indicates the phase space with the quadrupoles on, and the cross-hatched area the phase space with the quadrupoles off, showing immediately the much inferior momentum resolution. The desired product $\Delta p\Delta\theta_{\text{horizontal}}$ is obtained by integrating the the area of the phase-space curve. The vertical acceptance $\Delta\theta_{\text{vertical}}$ is obtained directly from Fig. 5(a). Finally, we must include the effect of finite target (or beam) size.

However, in spite of the straightforward nature of the calculation, in the present experiment the uncertainty in our estimate of the effective acceptance is 20% for the 0° and 32° spectrometers and 30% for the 17° one. The final values used in the reduction of our data are included in Table II.

In order to cross-check the calculated values we (a) compared the yield with the quadrupoles on and off,[19] and (b) measured experimentally the momentum resolution by observing known monochromatic lines. At 0° we used the pions[5] from $p+p\rightarrow d+\pi^+$ shown in Fig. 5(c) and obtain $dp/p=1.5\%$ full width at half-maximum. At 17° we measure the elastically scattered protons, where also the absolute cross section could be compared with the data of Cork *et al.*[20] As a final check, we have compared the pion yields deduced from this experiment with those measured earlier.[3] The over-all results are consistent within the uncertainty estimates given above.

[19] Appropriate collimators were introduced in order to maintain momentum resolution.

[20] B. Cork, W. Wenzel, and C. Causey, Phys. Rev. **107**, 859 (1957).

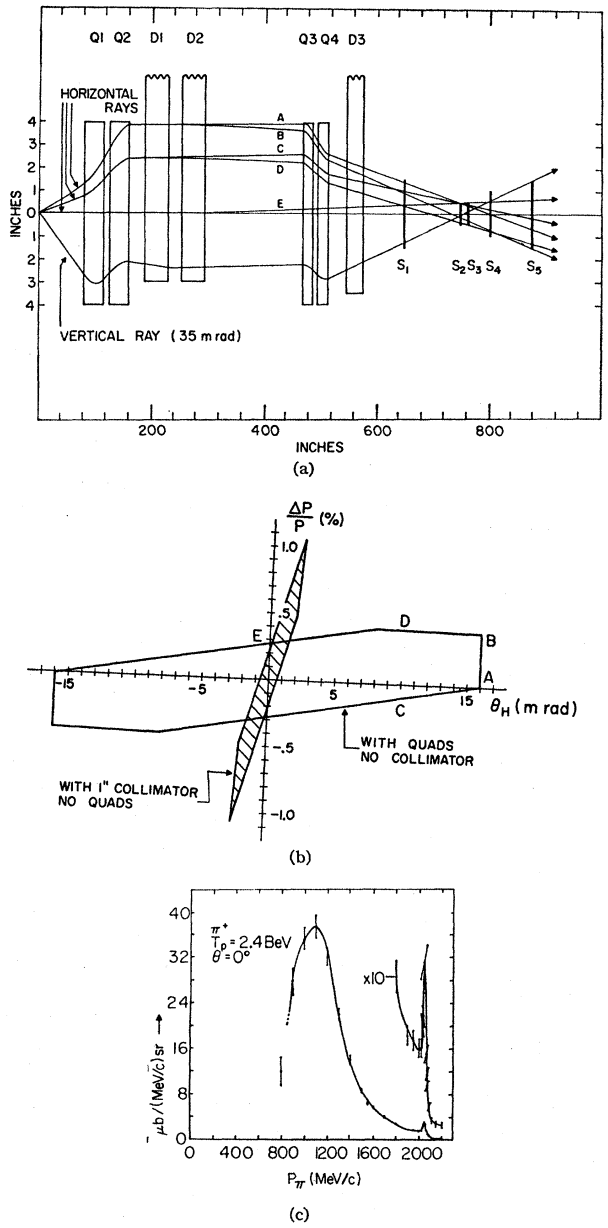

FIG. 5. Some characteristics of the 0° spectrometer. (a) Trace of the limiting vertical ray and of limiting horizontal rays. The position of the counters are also shown. (b) The phase-space diagram for the horizontal plane, resulting from the ray traces of (a) above. Note also the phase space with the quadrupoles turned off, which must now be limited by a 1-in. collimator in order to give acceptable momentum resolution. (c) The sharp peak in the π^+ spectrum from $p+p \rightarrow d+\pi^+$ at 0° is a measure of the resolution of the spectrometer, and is consistent with (b). The incident proton energy was 2.40 BeV.

The integrated flux incident onto the hydrogen target was obtained by the usual radiochemical method.[21] A polyethylene foil was exposed to the beam and the β^+ activity from the reaction $C^{12}(p,pn)C^{11}$ monitored. This yield was then related to a three-element telescope viewing the target at 90° to the beam, and which was used as the continuous monitor during data-taking.

III. EXPERIMENTAL RESULTS AND DISCUSSION

A. Results

The yield of K mesons obtained at each momentum was corrected, as explained in the previous section, for the following factors: (a) efficiency of detectors, (b) feed-through of π mesons, (c) absorption in detectors, (d) subtraction of the empty-target rate (which ranged from 2 to 8%), (e) solid-angle and momentum acceptance, (f) effective flux and target thickness, and (g) decay of K mesons.

Having applied these corrections, our data are in the form of the doubly differential cross sections shown in Figs. 6(a), 6(b), and 6(c) for $T_p=2.85$ BeV and Figs. 7(a) and 7(b) for $T_p=2.40$ BeV. The errors shown are a combination of the statistical error and the uncertainty in all corrections, except for the absolute normalization which introduces a 20–30% uncertainty common to all points, as discussed previously.[22] These results are also given in Tables IV and V for reference purposes.

A comparison of our results with those of other experimenters cannot be made directly. Dekkers *et al.*[23] reported on K^+ and K^- production in p-p collisions at 18.8- and 23.1-BeV/c incident energy. Piroué and Smith[24] reported on parts of the K^+ spectrum at 13°, 30°, and 93° in the laboratory in 2.9-BeV p-beryllium collisions.

A convenient procedure is to transform the laboratory spectra to the p-p center-of-mass system (c.m.s.). This is shown in Figs. 8(a), 8(b), 8(c), 9(a), and 9(b). At 0° the transformation to the c.m.s. again yields a momentum spectrum at fixed angle (obviously 0°); the contributions from slow K^+ mesons produced at 180° do not affect us, since the highest laboratory momentum which they can achieve is 600 MeV/c, which is below our detection limit. At 17° and 32° the c.m.s. angle varies with momentum as indicated by the upper scale in the figures. The transformation, however, is still unique, because of the cutoff in the lowest laboratory momentum measured.[25] The limit of the solid curves indicates the lowest c.m.s. momentum that can appear at the laboratory angle from which the data were transformed.

[21] J. B. Cummings, J. Hudis, A. Poskanzer, and S. Kaufman, Phys. Rev. 128, 2392 (1962).

[22] This error, however, is not necessarily the same for all angles.

[23] D. Dekkers, J. A. Geibel, R. Mermod, G. Weber, T. R. Willits, K. Winter, B. Jordan, M. Vivargent, N. M. King, and E. J. N. Wilson, Phys. Rev. 137, B962 (1965).

[24] P. A. Piroué and A. J. S. Smith, Phys. Rev. 148,1315(1966). These authors have also made measurements of K production in p-p collisions (to be published); see Ref. 36 of the paper referred to above.

[25] K mesons produced at backward angles in the c.m.s. when appearing at 17° or 32° in the laboratory will have momenta below our cutoff, even though their c.m.s. momentum falls in the region investigated.

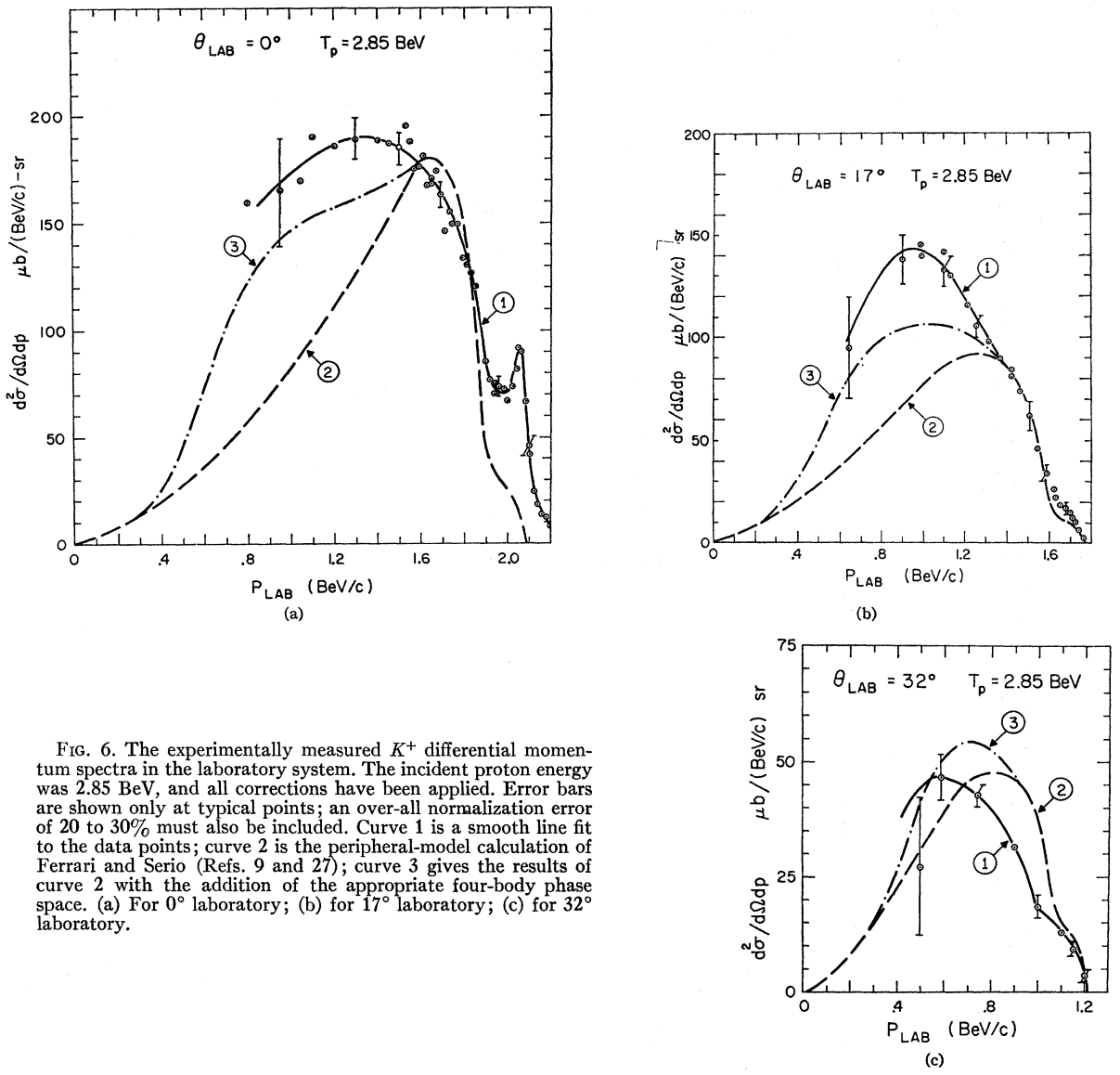

FIG. 6. The experimentally measured K^+ differential momentum spectra in the laboratory system. The incident proton energy was 2.85 BeV, and all corrections have been applied. Error bars are shown only at typical points; an over-all normalization error of 20 to 30% must also be included. Curve 1 is a smooth line fit to the data points; curve 2 is the peripheral-model calculation of Ferrari and Serio (Refs. 9 and 27); curve 3 gives the results of curve 2 with the addition of the appropriate four-body phase space. (a) For 0° laboratory; (b) for 17° laboratory; (c) for 32° laboratory.

It is clear from Figs. 8 and 9 that in this experiment we have covered almost the entire c.m.s. spectrum, in spite of the restriction of the laboratory measurements to K mesons of momenta greater than 600 MeV/c.

B. Comparison with Phase-Space Calculation

The c.m.s. spectra can be readily compared with the predictions of a simple phase-space calculation. The peak that occurs at the upper end of the spectrum, in particular at 0°, will be discussed in the following section.

We have used the expression given by Block[26] for three- and four-body phase space. The relative proportion of the contributing final states was taken from Louttit *et al.*,[6] and is also given below:

$$T_p=2.85 \text{ BeV}, \quad 0.40(p\Lambda K^+)+0.46(N\Sigma K^+)+0.14(YNK^+\pi);$$

$$T_p=2.40 \text{ BeV}, \quad 0.49(p\Lambda K^+)+0.49(N\Sigma K^+)+0.02(YNK^+\pi).$$

The ratios of the different production channels at $T_p=2.40$ BeV were obtained by scaling the $T_p=2.85$-BeV data on the basis of the available phase space.

The results of the phase-space calculation are shown in Figs. 8 and 9, where the experimental data are shown transformed to the c.m.s. We have chosen to normalize at each angle the phase space to the same area as the experimental curves, since our data are not compatible with isotropy in the c.m.s. The calculated momentum

[26] M. M. Block, Phys. Rev. **101**, 796 (1956).

TABLE IV. Laboratory momentum spectrum[a] of K^+ mesons produced in p-p collisions at an incident energy $T_p=2.85$ BeV.

(a) p_k(lab) (BeV/c)	0° laboratory angle $d^2\sigma/d\Omega dp$ [μb/(BeV/c) sr]	(b) p_k(lab) (BeV/c)	17° laboratory angle $d^2\sigma/d\Omega dp$ [μb/(BeV/c) sr]	(c) p_k(lab) (BeV/c)	32° laboratory angle $d^2\sigma/d\Omega dp$ [μb/(BeV/c) sr]
0.80	160[a]	0.64	95[a]	0.50	27[a]
0.95	166	0.90	138	0.59	47
1.05	170	0.99	142	0.74	43
1.10	191	1.10	138	0.90	32
1.20	186	1.14	130	1.00	19
1.30	190	1.22	116	1.10	13
1.40	189	1.26	106	1.15	10
1.45	188	1.32	98	1.20	3
1.50	186	1.37	90		
1.53	196	1.42	83		
1.55	189	1.46	74		
1.57	176	1.52	61		
1.59	177	1.56	46		
1.61	182	1.59	34		
1.63	168	1.62	25		
1.65	170	1.64	22		
1.67	175	1.65	18		
1.69	164	1.68	17		
1.71	147	1.70	16		
1.73	156	1.71	14		
1.75	150	1.72	11		
1.77	150	1.74	7		
1.79	134	1.76	4		
1.81	131				
1.83	127				
1.85	121				
1.90	86				
1.92	77				
1.94	71				
1.95	75				
1.96	74				
1.98	73				
2.00	67				
2.02	74				
2.04	82				
2.05	92				
2.06	91				
2.08	67				
2.10	44				
2.12	25				
2.14	19				
2.16	13				
2.18	12				
2.20	8				

[a] The relative errors on each point are as represented by the typical error bars in Fig. 6. An over-all systematic error in the absolute normalization of 20% for the 0° and 32° data and 30% for the 17° data must also be considered.

dependence seems to be a fair description of the experimental results even though the latter are shifted towards slightly higher energies.

C. Comparison with One-Meson-Exchange Calculations

In the last year, Ferrari and Serio[27] have performed a new calculation of strange-particle production in p-p collisions using the peripheral model,[9] with inclusion of one-pion and one-kaon exchange. They have also calculated the K^+ laboratory spectra relevant to the present experiment by considering the four graphs shown in Fig. 10.

As is well known, because of the much larger $Kp\rightarrow Kp$ cross section as compared with $\pi p\rightarrow KY$, the K-exchange graph would dominate. However, in their calculations, Ferrari and Serio have introduced a cutoff

$$F=[1+C(\Delta^2+\mu^2)]^{-1},$$

where C is an empirical parameter different for the pion and kaon graphs.

The usual expression for the differential spectra[28] was used:

$$\frac{d^2\sigma}{dT_2{}^L d\cos\theta_2{}^L}=\frac{q_2{}^L}{2\pi}\frac{G^2}{Mp_1{}^L}\frac{\Delta^2+(m_2-M)^2}{(\Delta^2+\mu^2)^2}k_1{}^Q\omega\sigma_1(\omega)F^2.$$

[27] We are grateful to Dr. E. Ferrari and S. Serio for permitting us to use their results prior to publication.

[28] See Ref. 9, Eq. (2.104).

Here

$$k_1{}^Q=[(1/4\omega^2)(\omega^2+M^2-\mu^2)^2-\mu^2]^{1/2},$$

ω is the total c.m. energy at the scattering vertex, μ is the mass of the exchanged particle, M is the proton mass, p^L, q^L are the three-momenta in the lab, and Δ^2 is the momentum transfer at the production vertex. $\sigma_1(\omega)$ is the on-mass-shell cross section for the scattering of the exchange particle at a total energy ω, and has been taken from the published data. $G^2=G_r^2/4\pi$, where G_r is the renormalized coupling constant, and the following values were used[29]:

$$G^2(NN\pi)=14.5,\quad G^2(N\Lambda K)=4.8\pm1.0,$$
$$G^2(N\Sigma K)=1.6\pm1.6.$$

The cutoff values, which could be considered as the only free parameters in the calculation, were obtained from an *over-all* fit to strange-particle production in p-p collisions up to 8 BeV/c. In particular, the total cross section for ΛpK^+ and the Δ^2 distributions were fitted.[7,8,30] The resulting values are $C(\pi)=(1/0.938)^2$ (BeV/c^2)$^{-2}$, $C(K)=(2/0.938)^2$ (BeV/c^2)$^{-2}$. With these parameters, the main contribution to the spectra comes from the pion graphs. The interference term arising from the permutation of the incident- and target-proton graphs has been computed only in S wave in K exchange.

The results of the one-meson-exchange calculation are shown in Figs. 6 and 7, together with the experimental points. We have also added the contributions

TABLE V. Laboratory momentum spectrum[a] of K^+ mesons produced in p-p collisions at an incident energy $T_p=2.40$ BeV.

(a) p_k(lab) (BeV/c)	0° laboratory angle $d^2\sigma/d\Omega dp$ [μb/(BeV/c) sr]	(b) p_k(lab) (BeV/c)	17° laboratory angle $d^2\sigma/d\Omega dp$ [μb/(BeV/c) sr]
0.80	71[a]	0.64	53[a]
0.90	102	0.75	82
1.05	123	0.84	84
1.10	138	0.93	86
1.20	144	0.98	98
1.26	152	0.99	104
1.28	144	1.10	96
1.30	153	1.14	90
1.35	151	1.20	76
1.38	122	1.22	72
1.40	115	1.25	44
1.45	82	1.28	32
1.48	79	1.32	31
1.50	80	1.35	27
1.52	82	1.36	24
1.53	96	1.37	24
1.54	90	1.40	13
1.56	103	1.42	4
1.58	77		
1.60	38		

[a] The relative errors on each point are as represented by the typical error bars in Fig. 7. An over-all systematic error in the absolute normalization of 20% for the 0° data and 30% for the 17° data must also be considered.

[29] M. Lusignoli, M. Restignoli, G. A. Snow, and G. Violini, Phys. Letters **21**, 229 (1966).

[30] G. Ascoli, M. Firebaugh, E. L. Goldwasser, V. E. Kruse, and R. D. Sard, in *Proceedings of the Thirteenth International Conference on High-Energy Physics, Berkeley, 1966* (University of California Press, Berkeley, 1967), abstract 9.a.6.

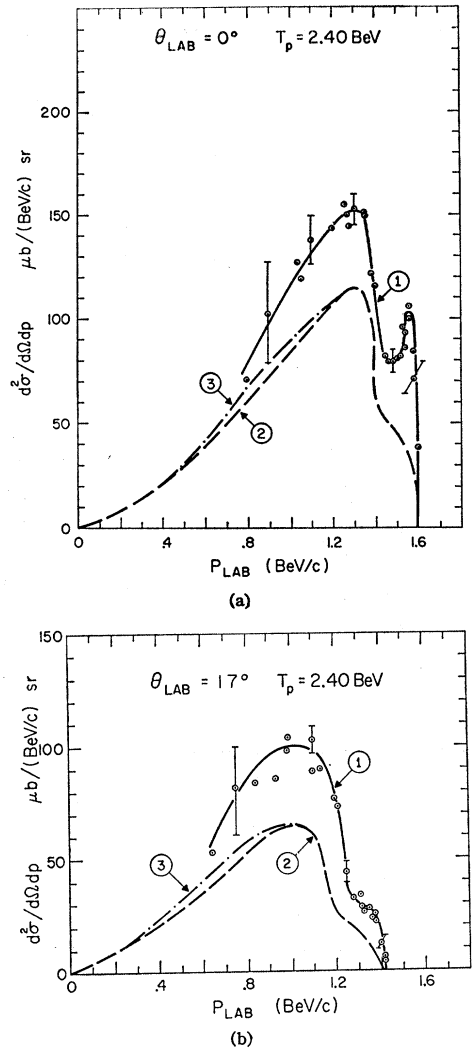

FIG. 7. Same as Fig. 6, but for an incident proton energy of 2.40 BeV. (a) For 0° laboratory; (b) for 17° laboratory.

of the four-body final states as obtained from phase space and the branching ratios given in the previous section.

Note that the agreement of the calculation and of the observed spectra is satisfactory at 0° and 32° for $T_p=2.85$, since no arbitrariness has been introduced in the absolute normalization. But even the 17° spectra are in reasonable agreement with the calculation; if one takes into account the 30% uncertainty in the absolute value of our own data and the contributions of the four-body final state, it is clear that the model is adequate at this level of experimental accuracy.

D. Angular Distributions and Total Cross Sections

By integrating the momentum spectra we can obtain points on the angular distribution for K^+ production in p-p collisions. The results are summarized in Table VI,

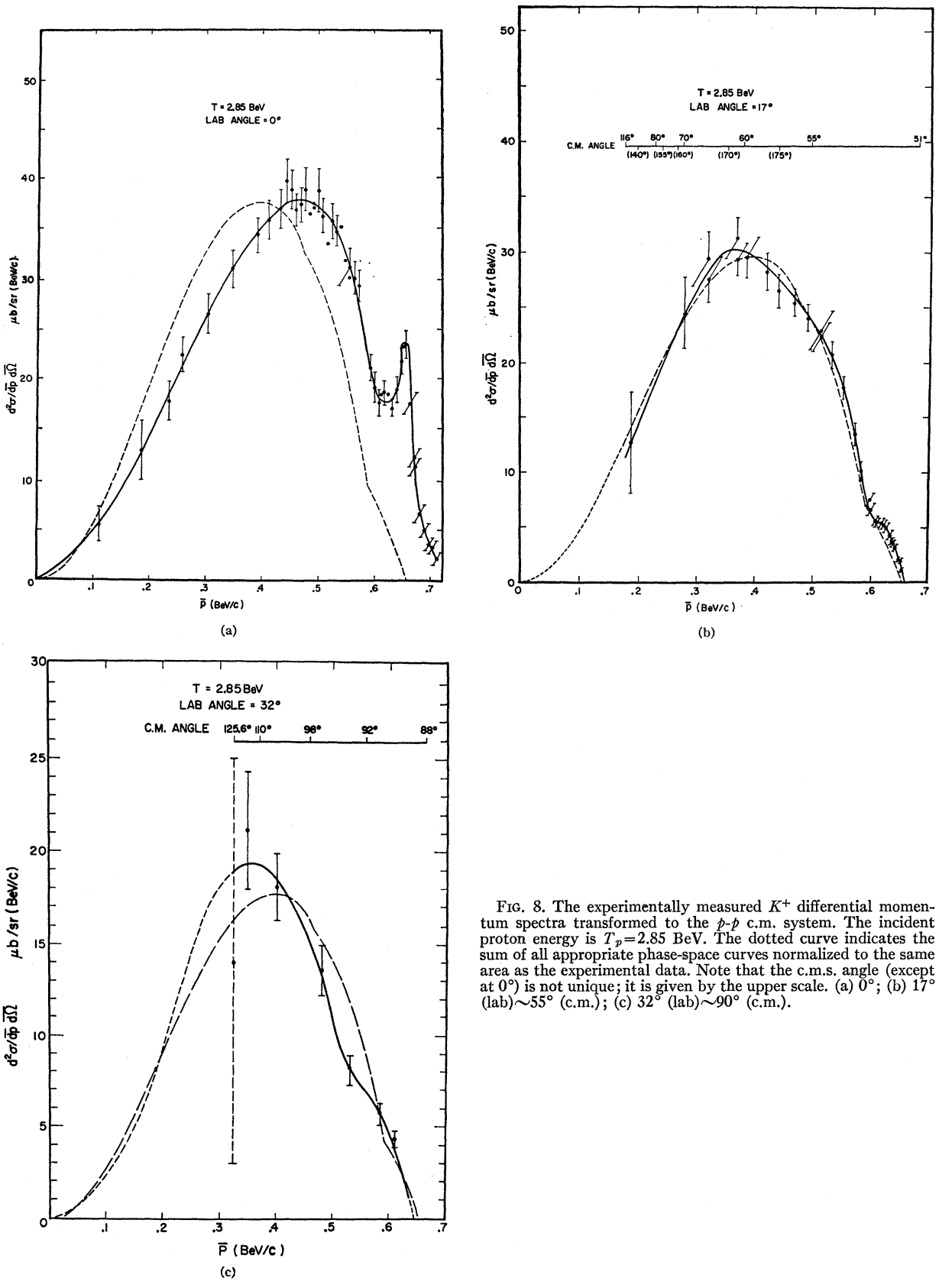

FIG. 8. The experimentally measured K^+ differential momentum spectra transformed to the p-p c.m. system. The incident proton energy is T_p=2.85 BeV. The dotted curve indicates the sum of all appropriate phase-space curves normalized to the same area as the experimental data. Note that the c.m.s. angle (except at 0°) is not unique; it is given by the upper scale. (a) 0°; (b) 17° (lab)∼55° (c.m.); (c) 32° (lab)∼90° (c.m.).

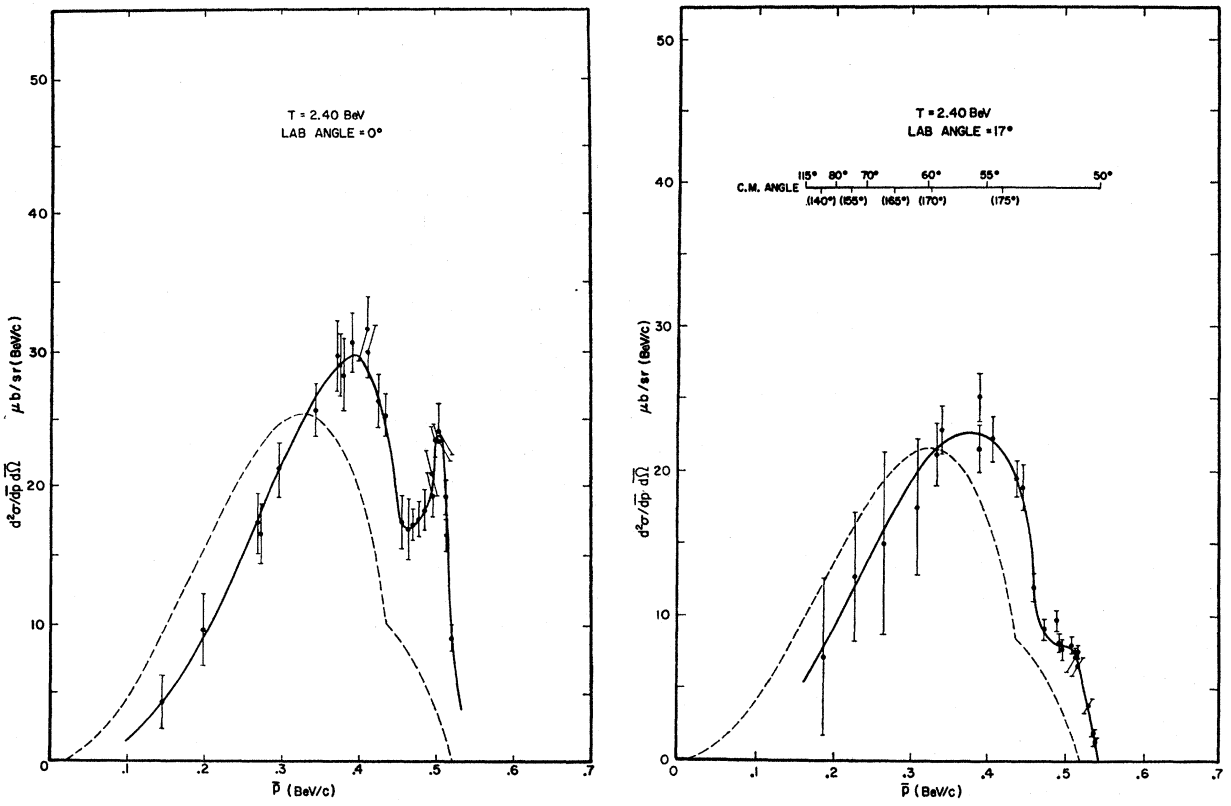

FIG. 9. Same as Fig. 8, but for an incident proton energy of 2.40 BeV. (a) 0°; (b) 17° (lab)~55° (c.m.).

both for the laboratory and the c.m.s. To arrive at a total cross section for K^+ production, we have made the simplest assumption (c.m.s. angular distribution as $A+B\cos^2\theta$) and obtained the results shown in Table VI. These results are lower than reported previously[4] because of a re-evaluation of the spectrometer acceptances (see Sec. II D).

We have estimated the contribution to the K^+-

TABLE VI. Angular distribution and total cross sections for K^+-meson production in p-p collisions.

Angular distribution $T_p=2.85$ BeV	
$d\sigma/d\Omega$ (lab)	$d\sigma/d\Omega$ (c.m.s.)
0° 272 ±55 μb/sr	0° 13.5± 2.8 μb/sr
17° 161 ±48 μb/sr	~55° 10.8± 3.0 μb/sr
32° 34.5± 8.0 μb/sr	~100° 6.5± 1.5 μb/sr
	$\sigma_T=126\pm30$ μb

Angular distribution $T_p=2.40$ BeV	
$d\sigma/d\Omega$ (lab)	$d\sigma/d\Omega$ (c.m.s.)
0° 116±23 μb/sr	0° 6.9± 1.5 μb/sr
17° 66±20 μb/sr	~58° 5.8± 1.8 μb/sr
	$\sigma_T=71$ ±18 μb

Comparison of total cross sections

Experiment[a]	p_p (BeV/c)	σ_T (μb)	Type of detector
1. This experiment	3.2	71± 18	Counters
	3.7	126± 30	Counters
2. Louttit *et al.*[b]	3.7	129± 25	Hydrogen bubble chamber
3. Bierman *et al.*[c]	5.0	200± 30	Hydrogen bubble chamber
4. Alexander *et al.*[d]	5.5	235± 50	Hydrogen bubble chamber
5. Ascoli *et al.*[e]	8.0	600±120	Hydrogen bubble chamber
6. Dekkers[f]	18.8	560±200	Counters

[a] In experiments 3 and 4 the contribution of channels without a Vee, such as $n\Sigma^+K^+$, $p\Sigma^-K^+\pi^+$, etc., is not given; it has been estimated by us and is included in the figures presented here.
[b] Reference 6. [c] Reference 7. [d] Reference 8. [e] Reference 30. [f] Reference 23.

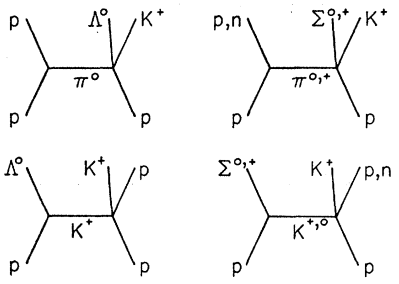

FIG. 10. The Feymnan graphs taken into consideration in the peripheral-model calculation.

production cross section from secondary processes, namely, a pion produced by the primary beam in the target interacts with another proton before leaving the target. From $p+p\rightarrow\pi^{+}+\cdots\rightarrow\pi^{+}+p\rightarrow K^{+}Y+\cdots$, we find an *upper* limit of 2.4% of the process $p+p\rightarrow K^{+}\cdots$; the $\pi^{-}p$ contribution is less than 0.2%. In view of the smallness of this effect, we have not applied any corrections for it.

Finally, in Table VI, we give a comparison of the total cross section for K^{+} production in p-p collisions as a function of incident energy.

At $T_p=2.85$ we detected a small number of K^{-} mesons produced at 0° with a laboratory momentum $p=1.1$ BeV/c. The ratio of $K^{-}/K^{+}=1/20$. Assuming a phase-space distribution and isotropy in the c.m.s., this corresponds to a total cross section $\sigma_T(pp\rightarrow K^{-}\cdots)=4\pm2\ \mu$b. No K^{+} mesons were observed above the $p\Lambda K^{+}$ threshold (i.e., from a possible reaction $p+p\rightarrow pnK^{+}$) with a confidence of a few μb; thus strangeness-nonconserving processes in the p-p collisions are suppressed by at least a factor of 100 with respect to the corresponding strangeness-conserving ones.

IV. LOW-ENERGY Λ-p INTERACTION

A. Phenomenological Analysis

At the upper limit of the K^{+}-momentum spectra, especially at 0°, we observe a distinct narrow peak[31] [see Figs. 6(a) and 7(a)]. Assuming a smooth extrapolation of the spectrum towards its cutoff, we estimate the following cross section (c.m.s.) for this effect: $d\sigma/d\Omega(0°)=0.25\pm0.10\ \mu$b/sr for $T_p=2.85$ BeV, and of the same order of magnitude for $T_p=2.40$ BeV. Since in this momentum region K^{+} mesons can only come from the $p\Lambda K^{+}$ final state, we conclude that the experimentally observed peak is a consequence of a singularity in the Λ-p scattering matrix in the vicinity of zero energy.

[31] At the 1965 Honolulu meeting of the American Physical Society, T. Elioff, C. M. Ankenbrandt, A. R. Clark, B. Cork, L. J. Kerth, and W. A. Wenzel reported observation of the same enhancement at 9.75° in the laboratory, with incident proton momenta of 4 and 5 BeV/c. They report that, even with improved (<1%) momentum resolution, the effect is less pronounced than our observation at 0° [Bull. Am. Phys. Soc. **10**, 717 (1965); also (private communication)].

Such a singularity can arise from the following three conditions: (a) the existence of a bound state (that would be a simple pole on the negative-energy axis), (b) the existence of a resonance (that would be a pole in the lower half of the complex plane close to the positive-energy axis), and (c) a strong Λ-p interaction at low positive energy (frequently referred to as a virtual state, and due to the existence of a pair of conjugate poles with respect to the imaginary axis, lying close to the real axis).

While the observation of such a manifestation of the Λ-p interaction is novel, its existence is not surprising. Both a direct measurement of Λ-p scattering[32,33] as well as the existence and study of hyperfragments[34] provide evidence for a strong Λ-p interaction.

In order to distinguish between the three above-mentioned possibilities, we first try to calculate the Q value of the Λ-p system corresponding to the peak in the K-meson spectrum. To reduce uncertainties related with the absolute value of the incident proton energy and spectrometer calibration, we use a comparison[35] of the K^{+} peak with the π^{+} peak from $pp\rightarrow d\pi^{+}$ (see Fig. 5). We obtain

$$Q=+4\pm8\ \text{MeV}/c^{2}.$$

The resolution on Q is not adequate to distinguish

TABLE VII. Low-energy scattering parameters for members of an SU_3 octet.

	Burnstein[a]	De Swart[b]	This experiment
Low-energy Λ-p interaction parameters			
a_s(singlet) F	−7.2	$-3.6_{-1.8}^{+3.6}$	$\lvert a\rvert=(3\pm1)$
r_{0s}(singlet) (F)	2	∼2	
a_t(triplet) (F)	−0.65	−0.53±0.12	
r_{0t}(triplet) (F)	5	∼5	
$\sigma_T(k\rightarrow0)$ (10^{-24} cm²)	1.65	0.41	1.13[c]
Low-energy N-N interaction parameters			
a_s(singlet) (F)	−23.7		
r_{0s}(singlet) (F)	2.5		
a_t(triplet) (F)	5.4		
r_{0t}(triplet) (F)	1.7		

[a] Reference 36.
[b] Reference 38.
[c] If we assume that $|a|$ is dominated by a_s we find $\sigma_T(k\rightarrow0)=4\pi a^2=0.28\times10^{-24}$ cm².

[32] B. Sechi-Zorn, R. A. Burnstein, T. B. Day, B. Kehoe, and G. A. Snow, Phys. Rev. Letters **13**, 282 (1964).
[33] G. Alexander, V. Karshon, A. Shapira, G. Yukutieli, R. Engelman, H. Filthuth, A. Fridman, and A. Minguzzi-Ranzi, Phys. Rev. Letters **13**, 484 (1964).
[34] See, for example, R. K. Adair, and E. C. Fowler, *Strange Particles* (Interscience Publishers, Inc., New York, 1963), pp. 82–84.
[35] For $\theta=0°$ we obtain

$$\frac{Q^2}{A}+\frac{2Q(m_\Lambda+m_p)}{A}+\frac{(m_\Lambda+m_p)^2-m_K^2}{A}=1-\frac{(E_K-E)-\bar{\beta}(p_K-p_\pi)}{m_p-E_\pi+\bar{\beta}p_\pi}.$$

Here $A=m_d^2-m_\pi^2$, and m_d is the mass of the deuteron, etc. E_k, E_π, etc., are the laboratory total energies where the K peak from ΛpK and the π peak from $pp\rightarrow d\pi^{+}$ occur; $\bar{\beta}$ is the p-p c.m.s. velocity. For more details, see J. T. Reed, thesis, University of Rochester, Rochester, N. Y., 1965 (unpublished).

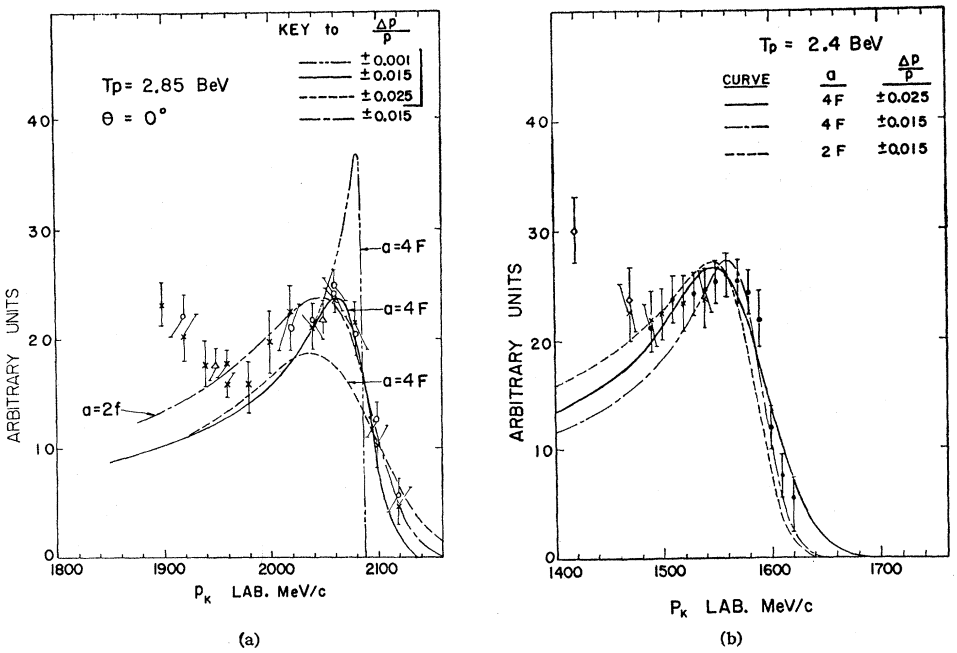

FIG. 11. Fitting of the upper end of the K^+ spectrum at 0° with a scattering-length formalism; see text for details. (a) Incident proton energy 2.85 BeV; (b) incident proton energy 2.40 BeV.

among the three possibilities, even though a positive Q value points against a bound state. Furthermore, the well-known extrapolation of the hyperfragment data[34] to $A=2, Z=1$ indicates that the Λ-p system is unbound by at least 1 MeV. Thus we reject the possibility of a bound state. Of the remaining two alternatives we favor the interpretation in terms of a final-state interaction. We are led to this by the fact that (a) the enhancement occurs essentially at zero relative Λ-p energy, (b) it can be fitted quite satisfactorily with the low-energy Λ-p-scattering parameters,[32,33,36] and (c) a Breit-Wigner fit to the peak yields a half-width

$$\tfrac{1}{2}\Gamma = 17_{-15}^{+10}\ \text{MeV}.$$

Thus in the case of a resonance its width would be larger than the Q value.

Adopting the interpretation in terms of a final-state interaction, we have fitted the data with an S-wave scattering formalism as given by Watson and Stuart.[37] Namely, we multiply the phase space by

$$[k^2+(1/a-\tfrac{1}{2}r_0k^2)^2]^{-1}, \tag{5}$$

where a is the scattering length and r_0 is the effective range; they are treated as variable parameters. k is the wave number corresponding to the relative momentum in the Λ-p rest system; finally, the over-all normalization is free. The results of the fit for the simplified case $r_0=0$ and $a=2$ and 4 F are shown in Figs. 11(a) and 11(b) for respective incident energies $T_p=2.85$ and 2.4 BeV. In comparing these calculations with experiment, it is essential to include the momentum resolution of the apparatus. Indeed, as can be seen from the figures, the leading edge of the spectrum provides a good measure of the experimental momentum resolution, indicating that $dp/p=1.5\%$, in agreement with our other independent estimates for it (see Table II). From both the $T_p=2.85$- and 2.40-BeV data we conclude that the best value of the one-parameter fit is

$$|a| = (3\pm1)\ \text{F}.$$

Use of a one-parameter fit to characterize the Λ-p interaction is clearly a simplification. Even when we consider only S states, the Λ-p system can be either in the triplet or singlet spin state, so that with the inclusion of effective range a total of four parameters is required. These are listed in Table VII, both as obtained from the Λ-p-scattering data[36] and from the analysis of hyperfragment binding energies.[38] The total cross section is then given by

$$\sigma_T(k)=\frac{\pi}{k^2+[(1/a_s)-\tfrac{1}{2}r_{0s}k^2]^2}+\frac{3\pi}{k^2+[(1/a_t)-\tfrac{1}{2}r_{0t}k^2]^2}. \tag{6}$$

Note that our independent determination of $\sigma_T(k\to 0)=4\pi a^2$ is in agreement with the other data[36,38] presented in Table VII.

Finally, in Fig. 12, we show the resulting fit to our K^+-meson spectrum when we use Eq. (6) above, with

[36] R. A. Burnstein, University of Maryland Technical Report No. 469, 1965 (unpublished).
[37] K. M. Watson and R. N. Stuart, Phys. Rev. **82**, 738 (1951).
[38] J. J. De Swart and C. Dullemond, Ann. Phys. (N.Y.) **19**, 458 (1962).

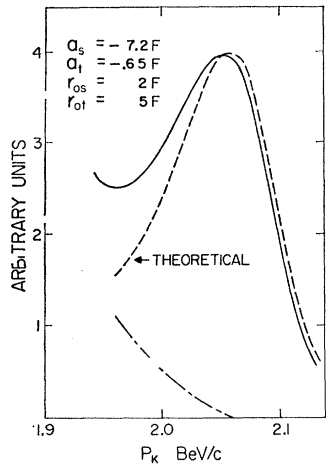

FIG. 12. Fitting of the upper end of the K^+ spectrum at 0° with an effective-range formalism, including both the singlet and triplet state. The parameters obtained from Λ-p scattering (Ref. 36) are used. Note that the theoretical curve (dashed) has been shifted for clarity. The dot-dash represents the difference of the experimental and theoretical curve. dp/p has been taken ±0.015.

the parameters obtained by Burnstein,[36] instead of Eq. (5). The fit is excellent, the theoretical curve (dashed) in Fig. 12 having been shifted for clarity. A m resolution of 1.5% has been included in the ca The difference between the experimental da curve) and the calculation is given by the d curve indicating the smooth rise of the undistorted K spectrum.

B. Discussion

In terms of $SU(3)$ symmetry, the Λ-p interaction can be related to the low-energy interaction of other baryon pairs belonging to the same octet.[39] The best-studied one, of course, is the nucleon-nucleon interaction for which the parameters shown in Table VII are applicable.

By combining two octets we can obtain the following representations:

$$8\otimes 8=1\oplus 8_s\oplus 8_a\oplus 10\oplus \bar{1}\bar{0}\oplus 27,$$

and the Λ-p system can belong to 8_s, 8_a, 10, or $\bar{1}\bar{0}$. In particular,

$$^3S_1(\Lambda p)=\tfrac{1}{2}\{\bar{1}\bar{0}\}+\tfrac{1}{2}\{8_a\},$$
$$^1S_0(\Lambda p)=(9/10)\{27\}+\tfrac{1}{10}\{8_s\},$$
$$^3S_1(pn\equiv d)=\{\bar{1}\bar{0}\},$$

so that from the present data we cannot uniquely determine the strength of the baryon-baryon interaction for each of the possible representations of the $8\otimes 8$ system.[40]

A related subject is the possibility of the existence of a resonant Λp (or, more generally, hyperon-nucleon) state. This would manifest itself as a peak in the K^+ spectrum if it is produced in p-p collisions with a detectable cross section. Other authors have reported on the possibility of the existence[41,42] of such a Λp state, with the following parameters:

$$Q\simeq 310\text{ MeV},\quad \Gamma=150\text{ MeV}\quad\text{(Ref. 41)};$$
$$Q=\ 45\text{ MeV},\quad \Gamma=\ 20\text{ MeV}\quad\text{(Ref. 42)}.$$

From our data we find no evidence for these states, and can place an upper limit for their production in p-p collisions at 6 μb/sr (laboratory) both at 0° and 17°. We also mention that a search for a possible bound or resonant $\Sigma^- n$ state by Davis *et al.*[43] gave negative results.

ACKNOWLEDGMENTS

/e are indebted to the staff of the Cosmotron, who le this experiment possible by their efficient opera- of the accelerator and of its support services. We are grateful for the continued support of the engineering and technical facilities of the University of Rochester and of Brookhaven National Laboratory. We wish to thank Dr. T. F. Kycia for the loan of his high-pressure differential Čerenkov counter, and Dr. E. Ferrari and S. Serio for permitting us to use the peripheral-model-calculation results before publication. We acknowledge the help of Dr. J. J. Russell, and of Dr. W. Metzger, R. Adelberger, S. Tewksbury, and T. Londergan with various phases of this experiment. Finally, it is a pleasure to thank H. Schulman for his valuable technical assistance.

[39] R. J. Oakes, Phys. Rev. **131**, 2239 (1963).

[40] A. Goldhaber and R. Socolow (private communication).

[41] R. A. Piroué, Phys. Rev. Letters **11**, 164 (1964).

[42] H. O. Cohn, K. H. Bhatt, and W. M. Bugg, Phys. Rev. Letters **13**, 668 (1964).

[43] H. R. Gustafson and H. F. Davis, Bull. Am. Phys. Soc. **12**, 104 (1967).